Geophysical Journal International

Geophys. J. Int. (2015) **201,** 915–928 doi: 10.1093/gji/ggv056
GJI Seismology

The runup on a multilinear sloping beach model

Mauricio A. Fuentes,[1,2] Javier A. Ruiz[1] and Sebastián Riquelme[3]

[1] *Department of Geophysics, Faculty of Physical and Mathematical Sciences, University of Chile, Santiago, Chile. E-mail: mauricio@dgf.uchile.cl*
[2] *Department of Mathematical Engineering, Faculty of Physical and Mathematical Sciences, University of Chile, Santiago, Chile*
[3] *National Seismological Center, Faculty of Physical and Mathematical Sciences, University of Chile, Santiago, Chile*

Accepted 2015 February 3. Received 2014 December 3; in original form 2014 April 28

SUMMARY

A general method of solution for the runup evolution and some analytical results concerning a more general bathymetry than a canonical sloping beach model are presented. We studied theoretically the water wave elevation and runup generated on a continuous piecewise linear bathymetry, by solving analytically the linear shallow water wave equations in the 1+1 dimensional case. Non-horizontal linear segments are assumed and we develop an specific matrix propagator scheme, similar to the ones used in the propagation of elastic seismic wave fields in layered media, to obtain an exact integral form for the runup. A general closed expression for the maximum runup was computed analytically via the Cauchy's residue Theorem for an incident solitary wave and isosceles leading-depression N wave in the case of $n + 1$ linear segments. It is already known that maximum run-up strongly depends only on the closest slope to the shore, although this has not been mathematically demonstrated yet for arbitraries bathymetries. Analytical and numerical verifications were done to check the validity of the asymptotic maximum runup and we provided the mathematical and bathymetrical conditions that must be satisfied by the model to obtain correct asymptotic solutions. We applied our model to study the runup evolution on a more realistic bathymetry than a canonical sloping beach model. The seabed in a Chilean subduction zone was approximated—from the trench to the shore—by two linear segments adjusting the continental slope and shelf. Assuming an incident solitary wave, the two linear segment bathymetry generates a larger runup than the simple sloping beach model. We also discussed about the differences in the runup evolution computed numerically from incident leading-depression and leading-elevation isosceles N waves. In the latter case, the water elevation at the shore shows a symmetrical behaviour in terms of theirs waveforms. Finally, we applied our solution to study the resonance effects due to the bathymetry modelled by linear segments, which is in agreement with published studies and numerical tests.

Key words: Fourier analysis; Non-linear differential equations; Tsunamis.

1 INTRODUCTION

On 2010 February 27, an M_w 8.8 mega-thrust earthquake broke 450 km length along the seismogenic contact interface of the Chilean subduction zone (Lay *et al.* 2010; Vigny *et al.* 2011; Hayes *et al.* 2013) in the south-central Chilean convergent margin; where the Nazca Plate subducts underneath the South American Plate. The tsunami generated by this event hit the Chilean coastal border along several hundred kilometres between Valparaíso and Valdivia cities (Fritz *et al.* 2011; Vargas *et al.* 2011). The largest peak-runup measured on the field reached 29 m at Constitución, and several eyewitnesses observed the arrival of destructive waves 2.5–4.5 hr after the origin time of the earthquake (Fritz *et al.* 2011; Vargas *et al.* 2011). These late waves were observed mainly along the coast of Biobío and Arauco regions. Yamazaki & Cheung (2011) attributed this effect to local bathymetry effects; in particular, they suggest trapped waves and amplification of energy over the continental shelf, resulting in resonance and local amplification. Ezersky *et al.* (2013) also investigated resonance of long wave over a continental shelf and slope bathymetry and have shown that bottom profiles influences the runup.

The recent major devastating tsunami generated by the 2011, M_w 9.0, Tohoku-Oki, Japan, mega-thrust earthquake occurred along the Japanese subduction zone (Mori *et al.* 2011; Wei *et al.* 2013), evidenced the need for a better understanding the tsunami generation process (Ide *et al.* 2011) related to the spatio-temporal complexity of coseismic earthquake ruptures and, in particular, its relationship with seismogenic subduction zones (Fujii *et al.* 2011). Tang *et al.* (2012) provide a method to estimate the energy transmitted by tsunami waves for unknown earthquake sources by using deep-ocean pressure measurements and numerical models, which provides important elements for near field forecast.

Some near-field tsunami effects are still not well understood, several factors control their generation, propagation and its effects on the shore, as inundation and run-up (Yamazaki & Cheung 2011; Kânoğlu *et al.* 2013).

Field survey of tsunamigenic earthquakes and the measurements of inundation and runup distribution along the coastline reveal that small-scale local bathymetric and geomorphological conditions might affect the runup height and the tsunami effects along the shore (e.g. Satake *et al.* 1993; Yeh *et al.* 1993; Mori *et al.* 2011; Vargas *et al.* 2011).

The estimate of runup and leading wave arrival times at the shore are among the most important parameters to be rapidly determined after a large near-shore tsunamigenic earthquake. Several theoretical and numerical models have been proposed and developed to better understand the tsunami generation, propagation and inundation processes (Kajiura 1970; Synolakis 1987, 1991; Yamazaki *et al.* 2009; Fuentes *et al.* 2013).

The canonical sloping beach model is the simplest bathymetry configuration broadly used to study runup and water wave evolution. In the long wave approximation, the shallow water wave equations are used to study this problem in the linear and non-linear approaches (Carrier & Greenspan 1958; Synolakis 1987; Carrier *et al.* 2003; Kânoğlu 2004; Kânoğlu & Synolakis 2006; Fuentes *et al.* 2013).

For instance, a sloping beach model was used to approximate—to first-order—the seafloor geometry of the Chilean subduction zone, to study theoretically the runup distribution along the shoreline in the 2+1 dimensional linear case (Fuentes *et al.* 2013). High-resolution bathymetry from research cruises and seismic reflection studies reveal clearly a spatially heterogeneous seafloor, however some major large-scale seabed features are observed from the trench to the shore, such as, the continental rise and slope, and continental shelf. The latter bathymetric feature mapped near-shore along the Maule and Biobío regions in Chile (Moscoso & Contreras-Reyes 2012) is characterized by a wide continental shelf that preserves a mild slope along the continental shelf. Certainly, all these seafloor observations confirm a more complex bathymetry rather than a simple sloping beach model, and also suggest that the approximation of the seabed by non-horizontal linear segments is a reasonable assumption. Then, when considering a 2-D profile orthogonal to the trench axis one might approximate the seabed by a continuous piecewise linear bathymetry.

Kânoğlu & Synolakis (1998) studied the 1+1 long wave evolution and runup on piecewise linear topographies analytically and experimentally to understand some coastal effects of tidal waves. Their results suggest that, at least for simple piecewise linear bathymetries, analytical methods can be used to calculate effectively some important physical parameters of long-wave runup. They proposed a general method of solution—including simultaneously horizontal and sloping segments—to retrieve the runup, but their analytical solution does not include a closed asymptotic expression for the maximum runup in the case of a bathymetry modelled by n linear segments but they solve explicitly the maximum runup only for some particular cases. Also Kânoğlu & Synolakis (1998) analysed runup on a conical island approximating the bathymetry by a collection of cylinders with different height and radius. These authors also give an extensive review of published works concerning water wave evolution on bathymetries different from the canonical sloping beach model. These authors proposed a general method for determining the time-series over piecewise linear bathymetries. They derive asymptotic results for the maximum runup of solitary waves only for particular cases of bathymetry. However, because they allow sloping and constant-depth segments to coexist in the same bathymetry model, these authors do not propose a general runup formula because the mathematical development becomes rather intractable.

Inspired by some major ocean bottom geometry features observed along the Chilean subduction zone, the aim of this work is to study theoretically the water wave elevation and runup generated on a piecewise linear bathymetry, by solving analytically the linear shallow water wave equations in the 1+1 dimensional case. We derived a closed form for the runup, assuming non-horizontal segments and we develop a matrix propagator scheme similar to the ones used in the propagation of elastic seismic wave fields in stratified media, such as, the well-known Haskell–Thompson method (Thomson 1950; Haskell 1953).

In the next sections, we will introduce briefly the linear shallow water wave equations and we start solving theoretically the water wave elevation and runup on a sloping beach model. Then, the solution method is generalized approximating the ocean bottom by a piecewise linear bathymetry and we will present the general expression for the runup. In both cases, the maximum runup is computed analytically in a closed form assuming an incident solitary wave and the isosceles leading-elevation N wave (Tadepalli & Synolakis 1994).

Analytical verifications and numerical test were done in order to check the validity of the asymptotic closed expression for the maximum runup and we discuss about the validity condition that must be satisfied to get correct asymptotic solutions. We also applied our results to study the runup on a more realistic bathymetry rather than a sloping beach model, approximating the seabed in a Chilean subduction zone by two linear segments. Numerical computations were done to compare the runup from both bathymetries assuming an incident solitary wave. Finally, we discuss the differences in the runup computed numerically from incident leading-depression and leading-elevation N waves.

2 BASIC THEORY AND EXISTING RESULTS

2.1 Governing equations

The non-linear shallow water wave equations in the 1+1 dimensional problem are,

$$\begin{aligned} &\eta_t + [(\eta + h)u]_x = 0 \\ &u_t + uu_x + g\eta_x = 0, \end{aligned} \tag{1}$$

where $\eta = \eta(x, t)$ is the water wave elevation over a datum level ($z = 0$), $h = h(x)$ is the bathymetry and $u = u(x, t)$ is the depth-integrated horizontal velocity.

The dimensional linearized version of set (1), retaining first-order terms is,

$$\begin{aligned} \eta_t + (hu)_x &= 0 \\ u_t + g\eta_x &= 0 \end{aligned} \tag{2}$$

but the equation system (2) can be written as an equivalent single second order partial differential equation (PDE) governing the water wave elevation,

$$\eta_{tt} - g(h\eta_x)_x = 0. \tag{3}$$

Synolakis (1987) has shown that the linear and non-linear approaches produce the same estimate of the runup in the case of a sloping beach model. Based in his conclusion, this work focuses on the linear theory and thus in solving eq. (3).

2.2 The sloping beach model

The sloping beach model is the simplest bathymetry model and has been broadly used in tsunami studies (Synolakis 1986, 1987, 1988; Tadepalli & Synolakis 1994, 1996; Okal & Synolakis 2004). It assumes a constant ocean depth domain joined to a linearly decreasing depth towards the shore. The bathymetry can be written as,

$$h(x) = \begin{cases} \tan(\beta)x & \text{if} \quad x \leq x_1 \\ d & \text{if} \quad x > x_1, \end{cases} \tag{4}$$

where d is the constant depth, β is the angle of the sloping beach and $x = x_1$ is the limit between the two domains. Fig. 1 shows the seafloor geometry, the origin of the coordinate system is located at the shoreline and x is positive seaward.

We use an integral transform method to solve the water wave elevation. The direct and inverse 1-D Fourier transform definitions used are, respectively,

$$\widehat{f}(\omega) = \int_{-\infty}^{\infty} f(t)\, \mathrm{e}^{-\mathrm{i}\omega t}\, \mathrm{d}t, \quad f(t) = \frac{1}{2\pi} \int_{-\infty}^{\infty} \widehat{f}(\omega)\, \mathrm{e}^{\mathrm{i}\omega t}\, \mathrm{d}\omega,$$

then eq. (3) can be transformed into a single equivalent ordinary differential equation (ODE) in the Fourier domain,

$$(h\widehat{\eta}_x)_x + k_0^2\, \mathrm{d}\widehat{\eta} = 0, \tag{5}$$

where $k_0 = \frac{\omega}{c_0}$ and $c_0 = \sqrt{gd}$ is the wave speed.

For the open sea, $x > x_1$, the general solution of the transformed eq. (5) is,

$$\widehat{\eta}(x, \omega) = A_I(\omega)\, \mathrm{e}^{\mathrm{i}k_0 x} + A_r(\omega)\, \mathrm{e}^{-\mathrm{i}k_0 x}, \tag{6}$$

where A_I and A_r represent the incident and reflection coefficients, respectively.

In the sloping beach domain, the variable substitution $\xi = 2k_0\sqrt{x x_1}$ transforms eq. (5) into a zero order Bessel equation. The general solution in this case is,

$$\widehat{\eta}(x, \omega) = B(\omega)J_0(\xi) + C(\omega)Y_0(\xi) \tag{7}$$

being $J_0(\,\cdot\,)$ and $Y_0(\,\cdot\,)$ the cylindrical Bessel functions of first and second kind, respectively. B and C are the transmitted coefficients or amplification factors. We seek for bounded solutions at the shore, thus C must be set to 0, because of the singularity of the Neumann function $Y(\,\cdot\,)$ at the origin. The bounded solution in the Fourier domain is,

$$\widehat{\eta}(\omega, t) = B(\omega)J_0\left(2k_0\sqrt{x x_1}\right). \tag{8}$$

Imposing continuity conditions at $x = x_1$ of the solutions (i.e. eqs 6 and 8) and their first partial derivative with respect to x, one retrieve the following set of equations,

$$A_I(\omega)\, \mathrm{e}^{\mathrm{i}k_0 x_1} + A_r(\omega)\, \mathrm{e}^{-\mathrm{i}k_0 x_1} = B(\omega)J_0(2k_0 x_1)$$

$$A_I(\omega)\, \mathrm{e}^{\mathrm{i}k_0 x_1} - A_r(\omega)\, \mathrm{e}^{-\mathrm{i}k_0 x_1} = -\mathrm{i}B(\omega)J_1(2k_0 x_1).$$

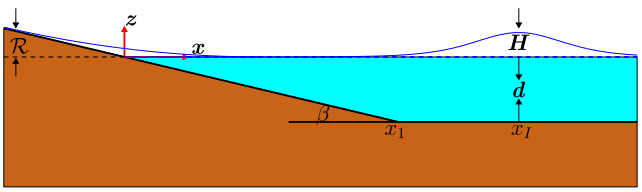

Figure 1. Sloping beach model.

This allows us to obtain,

$$A_r(\omega) = A_I(\omega)\, \mathrm{e}^{2\mathrm{i}\left[k_0 x_1 - \arctan\left(\frac{J_1(2k_0x_1)}{J_0(2k_0x_1)}\right)\right]} \tag{9}$$

$$B(\omega) = \frac{2A_I(\omega)\, \mathrm{e}^{\mathrm{i}k_0x_1}}{J_0(2kx_1) + iJ_1(2k_0x_1)}. \tag{10}$$

For a given boundary condition at the toe of the beach, $x = x_1$, expressed by its 1-D Fourier spectrum $\Phi(\omega)$, we can write the incident coefficient by the relation,

$$\widehat{\eta}(x_1, \omega) = A_I(\omega)\, \mathrm{e}^{\mathrm{i}k_0x_1} =: \Phi(\omega).$$

Finally, the transmitted solution to the sloping beach and evaluated at the shoreline ($x = 0$) is given by,

$$\eta(0, t) = \frac{1}{2\pi}\int_{-\infty}^{+\infty} \frac{2}{J_0(2k_0x_1) + iJ_1(2k_0x_1)}\Phi(\omega)\, \mathrm{e}^{\mathrm{i}\omega t}\, \mathrm{d}\omega \tag{11}$$

which is similar to the one given by Synolakis (1987).

2.3 Runup for an initial incident solitary wave

The solitary wave is the most regular exact solution from the Boussinesq equation (Boussinesq 1871), it means that the solution has a smooth profile, and fast decay of the wave amplitude and their high-order derivatives at the infinity. The solitary wave profile has the following expression,

$$\eta(x, t) = H\, \mathrm{sech}^2[\gamma(x - x_I + ct)], \tag{12}$$

where H is the maximum initial wave height, x_I is the initial centred location, $\gamma = \frac{1}{d}\sqrt{\frac{3H}{4d}}$ is a factor controlling the wavelength and $c = \sqrt{1 + \frac{H}{d}}c_0 := ac_0$ is the solitary wave speed, which is slightly greater than the linear tsunami wave speed, c_0. The latter effect is related to the non-linearity of the Boussinesq equation (Li & Raichlen 2001). This wave keeps the same shape when propagating, because the non-linear and dispersive effects are compensated.

The 1-D Fourier spectrum for this profile is given by (Synolakis 1987),

$$\Phi(\omega) = \frac{4d^3}{3}\frac{\pi}{c}\mathrm{e}^{\mathrm{i}k_c(x_1 - x_I)}k_c\, \mathrm{cosech}(\alpha k_c) \tag{13}$$

with $k_c = \frac{\omega}{c}$ and $\alpha = \frac{\pi}{2\gamma}$.

Inserting eq. (13) into eq. (11), and using the Cauchy's Residues Theorem and asymptotic expansions of the cylindrical Bessel functions, it is possible to obtain a closed formula for the maximum runup $\mathcal{R}$, maximizing $\eta(0, t)$ over t. The runup law is,

$$\mathcal{R} = 2.831H\left(\frac{H}{d}\right)^{\frac{1}{4}}\left(1 + \frac{H}{d}\right)^{\frac{1}{4}}\sqrt{\cot(\beta)}. \tag{14}$$

As discussed by Fuentes *et al.* (2013), this runup formula is slightly different from the one proposed by Synolakis (1987), due to the extra factor $(1 + \frac{H}{d})^{\frac{1}{4}}$ in eq. (14). It appears when solving a boundary value problem and the fact that the solitary wave speed is greater than c_0. The shallow water wave theory requires the ratio $\frac{H}{d}$ to be small, however the extra factor does not increase much the runup, because $\frac{H}{d}$ is usually less than 0.1 for non-breaking waves.

If $\frac{H}{d}$ is small, we can expand expression (14) to obtain

$$\mathcal{R} = \mathcal{R}_S + \mathcal{R}_C,$$

where $\mathcal{R}_S = 2.831H\left(\frac{H}{d}\right)^{\frac{1}{4}}\sqrt{\cot(\beta)}$ is the formula derived by Synolakis (1987) and $R_C = 0.708H\left(\frac{H}{d}\right)^{\frac{5}{4}}\sqrt{\cot(\beta)}$ can be interpreted as a correction term.

Notice that Li & Raichlen (2001) provide another correction term given by $R_{\mathrm{cr}} = 0.293H\left(\frac{H}{d}\right)^{\frac{5}{4}}\sqrt{\cot^3(\beta)}$. However R_C is a correction inside the linear regime, which actually in most of the cases can be neglected, instead R_{cr} is a correction for the non-linear contribution and it is more suitable for studying effects close to the shore.

2.4 Runup of isosceles *N* waves

The generalized *N* waves were introduced by Tadepalli & Synolakis (1994) to include a more realistic initial incoming tsunami wave shape. The isosceles *N* wave with elevation-subsidence waveform pattern is given by,

$$\eta(x, t) = -\frac{3}{2}\sqrt{3}H\, \mathrm{sech}^2[\gamma(x - x_I + ct)]\tanh[\gamma(x - x_I + ct)], \tag{15}$$

where $\gamma = \frac{3}{2d}\sqrt{\sqrt{\frac{3}{4}}\frac{H}{d}}$, H and x_I are defined as before. The 1-D Fourier spectrum for this profile can be easily computed using the solitary wave spectrum and Fourier transform properties,

$$\Phi(\omega) = -i\frac{3\sqrt{3}\pi H}{4c\gamma^3}k_c^2\,\mathrm{cosech}(\alpha k_c)\,\mathrm{e}^{\mathrm{i}k_c(x_1-x_I)}. \tag{16}$$

The runup in this case can be computed following the same mathematical formalism as the one used to retrieve the maximum runup of an incident solitary wave. It is given by,

$$\mathcal{R} = 3.861H\left(\frac{H}{d}\right)^{\frac{1}{4}}\left(1+\frac{H}{d}\right)^{\frac{1}{4}}\sqrt{\cot(\beta)}. \tag{17}$$

As shown in Section 2.3, we found again the extra factor, $\left(1+\frac{H}{d}\right)^{\frac{1}{4}}$, due to consider the c velocity in the wave evolution of the boundary value problem.

There is also a leading-depression N-wave profile (Tadepalli & Synolakis 1994). However, it is not possible to compute in a closed form the maximum runup following the mathematical formalism used here—that is using asymptotic expansions of cylindrical Bessel functions and complex countour integration—for a leading-depression N-wave pattern. The reason is that the series falls out of the convergence radius which leads to take the other complex half-plane where the kernel is not an entire function. There are few approaches to handle this (Tadepalli & Synolakis 1994, 1996; Madsen *et al.* 2010). However, let's point out that one can always compute numerically the water wave elevation at the shore using the integral expression (11), and then to evaluate the maximum from the time-series, $\eta(0, t)$.

3 PIECEWISE LINEAR BATHYMETRY MODEL

In order to include more realistic and important variations in the bathymetry, we consider a constant depth ocean domain followed by a continuous depth variation of $n\,(\geq 1)$ linear segments approaching the shore. We define a finite sequence of strictly decreasing points $\{x_i\}_{i=1}^{n+1}$, with $x_{n+1} = 0$ and theirs corresponding depths h_i, with $h_1 = d$ and $h_{n+1} = 0$. We do not use horizontal segments in the $[0, x_1]$ region, which means that the condition $h_i \neq h_{i+1}$, for $i = 1, \ldots, n$ must be used. We will show later that this condition allow us to retrieve an asymptotic closed form for the maximum runup in a general bathymetry of n linear segments. It is not a strong assumption because of the irregularity of real ocean bathymetries.

We define the following piecewise linear functions for the ocean bathymetry,

$$\begin{aligned} h_i(x) &= a_i + b_i x \quad i = 1, \ldots, n+1 \\ b_i &= \frac{h_i - h_{i-1}}{x_i - x_{i-1}}\ i = 2, \ldots, n+1,\ b_1 = 0 \\ a_i &= h_i - b_i x_i \quad i = 2, \ldots, n+1,\ a_1 = d, \end{aligned} \tag{18}$$

where b_i corresponds exactly to the slope of each segment. Fig. 2 sketches the general seafloor geometry using a piecewise linear bathymetry. As in the canonical sloping beach model, the origin of the coordinate system is located at the shore and x is positive seaward. It can be noticed, except for $i = 1$, that $b_i \neq 0$. Also, from the continuity relation for the ocean depth, the relation $h_i(x_i) = h_{i+1}(x_i)$ holds for $i = 1, \ldots, n$. This assumption follows the one proposed by Kânoğlu & Synolakis (1998), but we restrict our bathymetry to be described by sloping segments and continuous variation of the ocean depth.

3.1 General solution for the water wave elevation and runup evolution on a piecewise linear bathymetry

Similarly to the mathematical treatment done in the sloping beach case, the general equation governing the water wave elevation in the 1+1 linear problem is given by the transformed eq. (5). For a general linearly varying depth defined as $h(x) = a + bx$, the ODE becomes,

$$h(x)\widehat{\eta}_{xx} + b\widehat{\eta}_x + k_0^2\,\mathrm{d}\widehat{\eta} = 0,$$

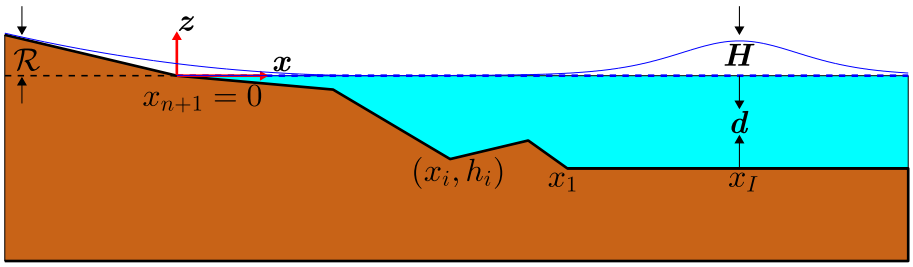

Figure 2. Piecewise linear bathymetry model.

and performing a change of variable, $\xi = 2k_0 \frac{\sqrt{dh(x)}}{|b|}$, the general solutions are zero order cylindrical Bessel functions of first and second kind,

$$\widehat{\eta}(x,\omega) = B(\omega)J_0(\xi) + C(\omega)Y_0(\xi), \tag{19}$$

and notice that ξ includes $|b|$, which means the previous solution is valid whether the segment slopes positively or negatively with respect to the horizontal constant depth of the open sea.

We can now define solutions at each inner linear depth segment as,

$$\begin{aligned}
\xi_i(x,\omega) &= 2k_0 \frac{\sqrt{\mathrm{d}h_i(x)}}{|b_i|} \qquad\qquad i = 2,\ldots,n+1 \\
\widehat{\eta}_i(x,\omega) &= B_i(\omega)J_0(\xi_i(x)) + C_i(\omega)Y_0(\xi_i(x)) \quad i = 2,\ldots,n+1,
\end{aligned} \tag{20}$$

where $\widehat{\eta}_1(x,\omega)$ is defined by eq. (6) (open sea domain) and B_i, C_i are the transmitted factors at each segment.

Now, we introduce the elevation-slope vector in the linear segment i defined by,

$$\mathbf{x}_i(x,\omega) = \begin{pmatrix} \widehat{\eta}_i(x,\omega) \\ \partial_x \widehat{\eta}_i(x,\omega) \end{pmatrix}, \tag{21}$$

where ∂_x denotes partial derivative with respect to x.

Let's define the following set of matrices for $i \geq 2$ (sloping segments) and the open sea domain,

$$\begin{aligned}
M_i(x,\omega) &= \begin{pmatrix} 1 & 0 \\ 0 & \sqrt{\frac{d}{h_i(x)}}k_0 \end{pmatrix} \quad i = 2,\ldots,n+1 \\
W_i(x,\omega) &= \begin{pmatrix} J_0(\xi_i) & Y_0(\xi_i) \\ J_0'(\xi_i) & Y_0'(\xi_i) \end{pmatrix} \quad i = 2,\ldots,n+1 \\
\mathbf{v}_i(\omega) &= \begin{pmatrix} B_i \\ C_i \end{pmatrix} \qquad\qquad i = 2,\ldots,n+1 \\
M_1 &= \begin{pmatrix} 1 & 0 \\ 0 & ik_0 \end{pmatrix} \\
W_1(x,\omega) &= \begin{pmatrix} \mathrm{e}^{\mathrm{i}k_0 x} & \mathrm{e}^{-\mathrm{i}k_0 x} \\ \mathrm{e}^{\mathrm{i}k_0 x} & -\mathrm{e}^{-\mathrm{i}k_0 x} \end{pmatrix} \\
\mathbf{v}_1(\omega) &= \begin{pmatrix} A_I \\ A_r \end{pmatrix},
\end{aligned} \tag{22}$$

where W_i is simply a Wronskian matrix. Definitions (22) allow us to write,

$$\mathbf{x}_i(x) = M_i(x)W_i(x)\mathbf{v}_i. \tag{23}$$

The continuity conditions of the solutions and their first derivatives with respect to x at each segment intersection, defined by the coordinate $x = x_i$, state,

$$\mathbf{x}_i(x_i) = \mathbf{x}_{i+1}(x_i), \quad i = 1,\ldots,n$$

which means that we can establish a relationship between the coefficients of adjacent segments $i+1$ and i, as,

$$\mathbf{v}_{i+1} = \Gamma_i \mathbf{v}_i, \tag{24}$$

where Γ_i is the matrix propagator from the linear segment i to $i+1$, given by,

$$\Gamma_i = W_{i+1}^{-1}(x_i)M_{i+1}^{-1}(x_i)M_i(x_i)W_i(x_i). \tag{25}$$

Setting the matrix $D_i =: M_{i+1}^{-1}(x_i)M_i(x_i)$, it implies,

$$\begin{aligned}
D_1 &= \begin{pmatrix} 1 & 0 \\ 0 & i \end{pmatrix} \\
D_i(x) &= I_2 \quad i = 2,\ldots,n+1,
\end{aligned} \tag{26}$$

where I_2 is the 2×2 Identity matrix. It is easy to show, by the continuity of the bathymetry, that,

$$\Gamma_1 = W_2^{-1}(x_1) D_1 W_1(x_1)$$

$$\Gamma_i = W_{i+1}^{-1}(x_i) W_i(x_i) \quad i = 2, \ldots, n. \tag{27}$$

Thanks to the recurrence relation (24), we can state a relationship between the transmitted, reflected and incident coefficients, from the constant ocean depth domain to the last segment,

$$\mathbf{v}_{n+1} = P \mathbf{v}_1, \tag{28}$$

where the 2×2 matrix P is the multiplication of all propagators,

$$P = \prod_{i=1}^{n} \Gamma_{n-i+1.} \tag{29}$$

Looking for a bounded solution at the shore, we must set $C_{n+1} = 0$, this allows to obtain easily from eq. (28) that,

$$A_r = -\frac{P_{21}}{P_{22}} A_I \tag{30}$$

$$B_{n+1} = \frac{\det(P)}{P_{22}} A_I. \tag{31}$$

One can make an extra algebraic effort using the properties of $\det(\cdot)$, the telescopic product and the Wroskian identity for Bessel functions, $\det[W_{i+1}(x_i)] = \frac{2}{\pi \xi_{i+1}(x_i)}$, to obtain in a closed form,

$$\det(P) = -2\pi i k_0 \mathrm{d} \sqrt{\frac{1}{|b_{n+1}|}}. \tag{32}$$

Now and forward, we still call B_{n+1} to the factor without the incident coefficient, that is $B_{n+1} = \frac{\det(P)}{P_{22}}$.

Similarly to the sloping beach case, providing an incident wave and its 1-D Fourier spectrum given by the boundary condition at $x = x_1$, the transmitted water wave elevation solution evaluated at the shore is,

$$\eta(0, t) = \frac{1}{2\pi} \int_{-\infty}^{+\infty} B_{n+1}(\omega)\, \mathrm{e}^{-\mathrm{i}k_0 x_1}\, \Phi(\omega)\, \mathrm{e}^{\mathrm{i}\omega t} \mathrm{d}\omega. \tag{33}$$

3.2 Validation of the general solution for some specific bathymetry cases

The theoretical generalized solution retrieved for the water wave elevation on a piecewise linear bathymetry model should reproduce exactly the same solution as the sloping beach case. There are two ways to verify this.

3.2.1 Simplest case: $n = 1$

We can write the linear depth segment in terms of the sloping beach angle as $h_2(x) = \cot(\beta)x$, which means that $\xi_2(x) = 2k_0\sqrt{x x_1}$.

The matrix P is reduced only to one propagator, that is $P = \Gamma_1$, and is given by

$$P = \frac{1}{\det(W_2(x_1))} \begin{pmatrix} [Y_0'(\xi_2(x_1)) - i\, Y_0(\xi_2(x_1))]\, \mathrm{e}^{ik_0 x_1} & [Y_0'(\xi_2(x_1)) + i\, Y_0(\xi_2(x_1))]\, \mathrm{e}^{-ik_0 x_1} \\ [-J_0'(\xi_2(x_1)) + i\, J_0(\xi_2(x_1))]\, \mathrm{e}^{ik_0 x_1} & [-J_0'(\xi_2(x_1)) - i\, J_0(\xi_2(x_1))]\, \mathrm{e}^{-ik_0 x_1} \end{pmatrix} \tag{34}$$

Using eq. (30), one can verify that expressions (28) and (29) are exactly the same than eqs (9) and (10), so we obtain the same solutions than the ones from the sloping beach model.

3.2.2 Arbitrary collinear control points

Choosing linearly decreasing collinear $\{h_i\}_{i=1}^n$ depths defining linear segments with the same sloping angle β, we can write $h_i = \cot(\beta)x_i$, $i = 1, \ldots, n+1$, which implies $\xi_i = 2k_0\sqrt{x x_i}$, $i = 2, \ldots, n+1$. This result allows to simplify the matrix (27), because $\Gamma_i = I_2$ for $i = 2, \ldots, n$, so, $P = \Gamma_1$ and the same process applied in Section 3.2.1 can be used here, thus obtaining the same solution as the sloping beach model as we expected.

3.2.3 Physical consistency of the solution

A first physical intuition is that using linear theory, the reflection coefficient over the open sea should remain the same incident amplitude but only differing by a phase change. Splitting the P matrix as follow,

$$P = \underbrace{W_{n+1}^{-1}(x_n)W_n(x_n)\cdots W_2(x_2)W_2^{-1}(x_1)}_{:=N}\underbrace{D_1 W_1(x_1)}_{=:L},$$

it is possible to show that

$$P = \begin{pmatrix} [N_{11} + iN_{12}]\,\mathrm{e}^{ik_0x_1} & [N_{11} - iN_{12}]\,\mathrm{e}^{-ik_0x_1} \\ [N_{21} + iN_{22}]\,\mathrm{e}^{ik_0x_1} & [N_{21} - iN_{22}]\,\mathrm{e}^{-ik_0x_1} \end{pmatrix}$$

and using eqs (30) and (31), one finds,

$$B_{n+1} = \frac{\det(P)}{N_{21} - iN_{22}}\mathrm{e}^{ik_0x_1}A_I$$

$$A_r = e^{2i\left(k_0x_1 - \arctan\left(\frac{N_{21}}{N_{22}}\right)\right)}A_I, \tag{35}$$

then obtaining what we expected, that is $\frac{|A_r|}{|A_I|} = 1$, which means that the reflected wave on the open sea preserves its amplitude.

3.2.4 Mathematical consistency of the solution

On the other hand, the Fourier inversion process to retrieve the water wave elevation at the shore must return a real valued solution. To show this, notice that eq. (32) can be split and written as,

$$\eta(0,t) = \frac{1}{2\pi}\int_0^{+\infty}[B_{n+1}(\omega)\Phi(\omega)\,\mathrm{e}^{-ik_0x_1}\mathrm{e}^{i\omega t} + B_{n+1}(-\omega)\overline{\Phi}(\omega)\,\mathrm{e}^{ik_0x_1}\mathrm{e}^{-i\omega t}]\,\mathrm{d}\omega \tag{36}$$

Here we use the complex conjugate property, $\Phi(-\omega) = \overline{\Phi}(\omega)$, because Φ comes from the Fourier transform of a real function (the water elevation η at x_1 in this case). So, the claim is that $B_{n+1}(-\omega) = \overline{B}_{n+1}(\omega)$. To see this, we can use the following matrix decomposition,

$$P = K\Gamma_1,$$

where $K = \prod_{i=1}^{n-1}\Gamma_{n-i+1}$ and Γ_1 is exactly eq. (32). Due to the parity of Bessel functions,

$$W_i(x_i, -\omega) = EW_i(x_i, \omega), \quad i = 2, \ldots, n+1,$$

where $E = \left(\begin{smallmatrix} 1 & 0 \\ 0 & -1 \end{smallmatrix}\right)$ is an elementary matrix. It is straightforward to verify, $W_i^{-1}(x_i, -\omega) = W_i^{-1}(x_i, \omega)E^{-1}$, $i = 2, \ldots, n+1$, and this simple fact allows us to prove that the propagator matrices satisfy,

$$\Gamma_i(-\omega) = \Gamma_i(\omega), \quad i = 2, \ldots, n+1.$$

Finally it can be noticed from eq. (31) that $\Gamma_1(-\omega) = \overline{\Gamma}_1(\omega)$ (conjugation in each matrix component), what implies that $B_{n+1}(-\omega) = \overline{B}_{n+1}(\omega)$, proving our claim. With this, eq. (34) can be expressed as,

$$\eta(0,t) = \frac{1}{\pi}\mathrm{Re}\left\{\int_0^{+\infty}B_{n+1}(\omega)\Phi(\omega)\,\mathrm{e}^{-ik_0x_1}\mathrm{e}^{i\omega t}\mathrm{d}\omega\right\} \tag{37}$$

obtaining a real valued solution as we expected.

3.3 Calculation of a general runup for a piecewise linear bathymetry model

In this section, we focus on obtaining an analytical closed form for the maximum runup on a piecewise linear bathymetry, in order to establish some physical dependences of the runup with the model parameters. We compute analytically the runup integral (31) by using the Cauchy's residues theorem, considering the 1-D Fourier spectrum of two kinds of incoming waves: (a) solitary wave and (b) isosceles N waves, with spectra given by expressions (13) and (16), respectively.

In our mathematical development, we adopt the conjecture proposed by Kânoğlu & Synolakis (1998); that is to say, we assume that $B_{n+1}(\omega)$ is an entire function in the lower complex half-plane, that is it has no zeros in that region. We can rewrite (31) changing the variable of integration ω to take in advantage the dependence with the wavenumber k_c,

$$\eta(0,t) = \frac{c}{2\pi}\int_{-\infty}^{+\infty}B_{n+1}(ck_c)\Phi(ck_c)\,\mathrm{e}^{ik_c(ct - ax_1)}\mathrm{d}k_c \tag{38}$$

being $a = \sqrt{1 + \frac{H}{d}}$.

Notice that in both studied cases (Solitary and N wave), the poles in the complex plane of the kernel in (36), are the poles of cosech(αz), which are $z_m = -i\kappa_m$, with $\kappa_m = \frac{m\pi}{\alpha}$ for $m \in \mathbb{N}$. It can be easily computed that the residue of this function is $\frac{(-1)^m}{\alpha}$.

Using asymptotic expansions of cylindrical Bessel functions for large arguments,

$$J_0(z) \approx Y_1(z) \approx \sqrt{\frac{2}{\pi z}} \cos\left(z - \frac{\pi}{4}\right)$$

$$J_1(z) \approx Y_0(z) \approx \sqrt{\frac{2}{\pi z}} \sin\left(z - \frac{\pi}{4}\right) \tag{39}$$

the Wronskian matrices can be written as,

$$W_i(x) \approx \frac{\mathrm{e}^{w_{m,i}}}{\sqrt{2\pi w_{m,i}}} A, \tag{40}$$

where $w_{m,i}(x) = 2a\kappa_m \frac{\sqrt{\mathrm{d}h_i(x)}}{|b_i|}$, $A = \left(\begin{smallmatrix} 1 & -i \\ i & -1 \end{smallmatrix}\right)$ and it is easy to verify that $A^{-1} = \frac{1}{2}A$.

Eq. (37) allows us to write the propagators,

$$\Gamma_i \approx \left(\frac{|b_i|}{|b_{i+1}|}\right)^{\frac{1}{2}} \mathrm{e}^{2a\kappa_m \sqrt{\mathrm{d}h_i}\left(\frac{1}{|b_i|} - \frac{1}{|b_{i+1}|}\right)} I_2. \tag{41}$$

Looking back to Section 3.2.3 and the P matrix expression, we can use eq. (39) and the telescopic summation property to obtain,

$$N \approx |b_{n+1}|^{-\frac{1}{2}} \sqrt{2\pi a \mathrm{d}\gamma m}\, \mathrm{e}^{4a\mathrm{d}\gamma m\left[\sum_{i=2}^{n} \sqrt{\frac{h_i}{d}}\left(\frac{1}{|b_i|} - \frac{1}{|b_{i+1}|}\right) - \frac{1}{|b_2|}\right]} A \tag{42}$$

which produces an explicit approximate expression for B_{n+1},

$$B_{n+1} \approx 2\sqrt{\pi a m \sqrt{3}} \left(\frac{H}{d}\right)^{\frac{1}{4}} |b_{n+1}|^{-\frac{1}{2}} \mathrm{e}^{2a\gamma x_1 m} \mathrm{e}^{-4a\gamma \mathrm{d} l_n m} \tag{43}$$

with $l_n = \frac{1}{|b_2|} - \sum_{i=2}^{n} \sqrt{\frac{h_i}{d}} \left(\frac{1}{|b_i|} - \frac{1}{|b_{i+1}|}\right)$.

3.3.1 Runup for an initial incident solitary wave

We use the Fourier spectrum (13) for the solitary wave, and the Cauchy's residues theorem in the convergence region to obtain the runup,

$$\eta(0,t) = 8\sqrt{\pi\sqrt{3}} H \left(\frac{H}{d}\right)^{\frac{1}{4}} \left(1 + \frac{H}{d}\right)^{\frac{1}{4}} |b_{n+1}|^{-\frac{1}{2}} \sum_{m=1}^{\infty} (-1)^{m+1} m^{\frac{3}{2}} \mathrm{e}^{2\gamma m(x_1 - x_I + ct - 2a\mathrm{d}l_n)} \tag{44}$$

taking the maximum value of this series, as done in Synolakis (1987), we find the maximum runup and the time of the maximum,

$$\mathcal{R} = 2.831 H \left(\frac{H}{d}\right)^{\frac{1}{4}} \left(1 + \frac{H}{d}\right)^{\frac{1}{4}} |b_{n+1}|^{-\frac{1}{2}}$$

$$t_{\max} = \frac{1}{c}\left(x_I + 2a\mathrm{d}l_n - x_1 - \frac{0.366}{\gamma}\right). \tag{45}$$

The runup amplitude is again modulated by the extra factor $(1 + \frac{H}{d})^{\frac{1}{4}}$. It is worth noting, that the runup law depends only on the slope of the last segment. However, it is important to remark that this runup law is valid under the validity range of the asymptotic expansions of the Bessel functions for large arguments.

3.3.2 Runup for an isosceles N wave

We use the Fourier spectrum of an isosceles leading-elevation N wave (16), and following the same mathematical development done in Section 3.3.1, we obtain the runup,

$$\eta(0,t) = 36\sqrt{\pi}\left(\frac{3}{4}\right)^{\frac{1}{8}} H \left(\frac{H}{d}\right)^{\frac{1}{4}} \left(1 + \frac{H}{d}\right)^{\frac{1}{4}} |b_{n+1}|^{-\frac{1}{2}} \sum_{m=1}^{\infty} (-1)^{m+1} m^{\frac{5}{2}} e^{2\gamma m(x_1 - x_I + ct - 2a\mathrm{d}l_n)} \tag{46}$$

and evaluating this expression at the maximum of the series, we obtain the maximum runup and the time at which it is reached,

$$\mathcal{R} = 3.861 H \left(\frac{H}{d}\right)^{\frac{1}{4}} \left(1 + \frac{H}{d}\right)^{\frac{1}{4}} |b_{n+1}|^{-\frac{1}{2}}$$

$$t_{\max} = \frac{1}{c}\left(x_I + 2a\mathrm{d}l_n - x_1 - \frac{0.914}{\gamma}\right). \tag{47}$$

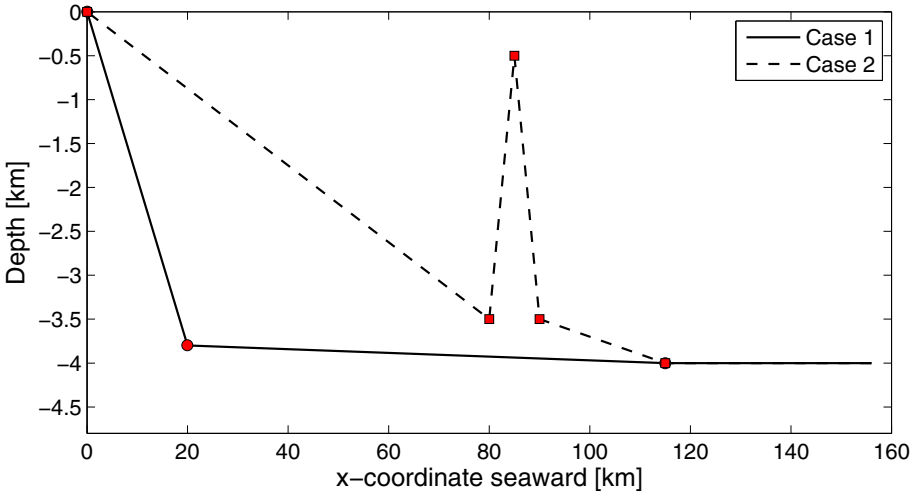

Figure 3. Two examples of a bathymetry in which the asymptotic maximum runup formula fails to estimate the exact maximum value.

This runup formula provides a larger value than the runup estimated from an incident solitary wave, conclusion already pointed out in other studies (Tadepalli & Synolakis 1994, 1996). The runup also strongly depends only on the slope of the last segment, and the model parameter dependence is similar to the solitary wave case.

If one considers, a leading-depression N wave, the runup must be computed numerically using the integral expression. In the next section, we show some numerical examples.

3.4 Numerical tests and examples of runup modelling

We present some numerical examples of the runup computed in a more realistic bathymetry than the canonical sloping beach model. We set some specific parameters to represent the seafloor geometry of a cross-section ortogonal to the trench-axis of a typical Chilean subduction zone. The sloping beach model can be roughly approximated—to first-order—as, $d = 4$ km, $x_1 = 115$ km, where the constant-depth, d, is the average ocean depth and x_1 is the distance from the coastline to the trench. The initial incident wave is located at $x_I = 130$ km , and the initial wave height is kept unchanged to $H = 5$ m. Over this fixed seafloor geometry, that is keeping x_1 and d fixed, we introduce a more representative bathymetry of a Chilean subduction zone approximating the seafloor, from the trench to the shoreline, by two linear segments which are intended to describe the continental slope and continental shelf.

3.4.1 Validity range of the runup law

The runup integral formula (32) provides the exact solution for the water wave elevation at the shore on a piecewise linear bathymetry, for any incident wave profile. In the mathematical derivation of the runup law, one can find examples of bathymetries where the asymptotic theoretical solution fails to predict the exact maximum runup value. It is because the asymptotic expansion of the cylindrical Bessel functions for large arguments are not valid anymore. The validity range of the asymptotic forms are true when at each segment the inequality $4a\gamma \frac{\sqrt{\mathrm{d}h_i}}{|h_{i+1}|} \gg 0.75$ holds $\forall i = 1 \ldots n$, (if it is greater than 2, the approximation error is less than 5 per cent). If there is at least one segment where the inequality does not hold true, the runup law does not estimate correctly the maximum runup.

We present examples of two bathymetries sketched in Fig. 3 where the inequality fails, basically because there are some linear segments with steep slopes. We use an incident solitary wave to model the runup. In the first case (solid line), the runup and maximum time pair estimated from the asymptotic forms are (6.11 m, 9.12 min), respectively. Instead, the ones computed numerically from the exact integral form are (10.33 m, 11.24 min), thus the asymptotic forms underestimate both values. The second case (dashed line) presents larger differences. The results obtained are, (12.73 m, 14.14 min) from the asymptotic closed forms, and (27.26 m, 14.36 min) computed numerically from the integral expression.

3.4.2 Comparison of the runup for sloping beach and two-linear-segment bathymetries

Fig. 4(a) shows the comparison between a sloping beach and a more realistic bathymetry for a typical Chilean subduction zone. The two-linear-segment seafloor geometry delimits the continental rise and slope (one segment) and the continental shelf (second segment) in a Chilean subduction zone. High resolution bathymetries evidence a continental slope steeper than the continental shelf, where the last segment approaching the shore is characterized by a mild slope at Maule and Biobío regions (Moscoso & Contreras-Reyes 2012).

The water wave elevation at the shoreline is computed for both bathymetries using an incident solitary wave (Fig. 4d). In the sloping beach case, the maximum runup computed numerically from the integral expression (37) is 15.36 m reached at 16.86 min, whereas the theoretical formulas (44) predict a runup of 14.28 m reached at 16.92 min.

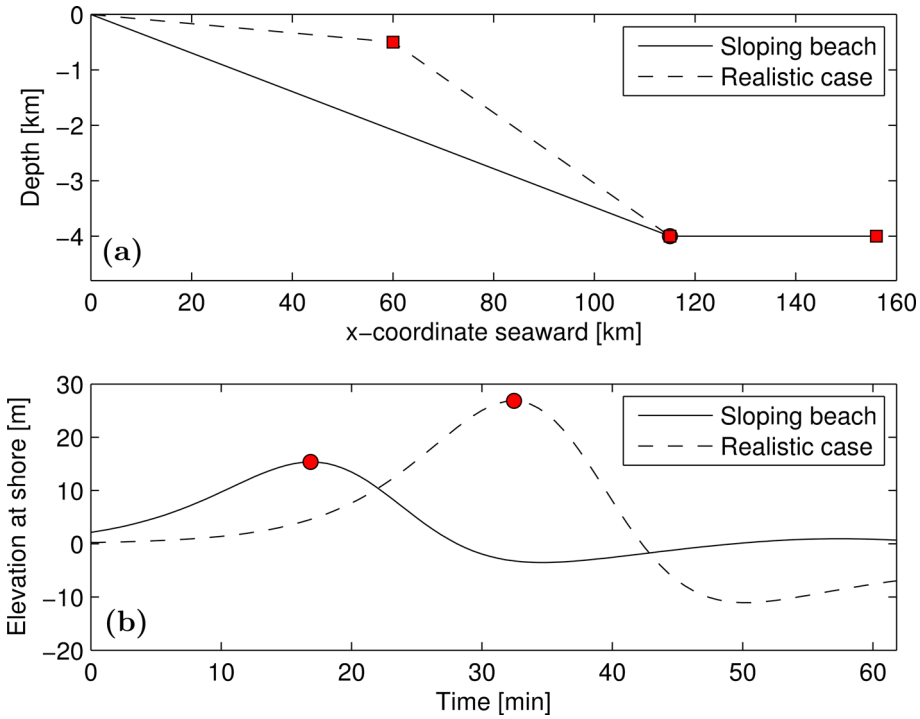

Figure 4. Runup comparison for two bathymetry settings where the seafloor in a typical Chilean subduction zone is approximated by a sloping beach and a two linear segments geometry. (a) Two bathymetries. (b) Runup evolution at the shore.

Instead, in a realistic bathymetry, the numerical solution obtained from the integral form provides 26.83 m and 32.46 min, for the runup and maximum runup time, respectively. The asymptotic closed solutions predict 29.17 m for the runup and 32.46 min for the maximum time. In both maximum runup predictions, we found a good agreement between the numerical and analytical solutions.

However, the runup comparison for these seafloor geometries, shows that a realistic bathymetry produces an asymptotic runup much more larger than the one generated by a canonical sloping beach model. It is basically because the last segment of the two linear bathymetry has a mild slope compared to the sloping beach. This difference in the maximum runup can be easily explained from the analytical runup law by obtaining a scaling relationship. If we keep the same initial incident wave, same wave height H and average ocean depth d, but analysing two different bathymetries where the runup law is valid, let's say by (1) and (2), and shaped by $n+1$ and $m+1$ linear segments, respectively, it holds the runup ratio,

$$\frac{\mathcal{R}^{(1)}}{\mathcal{R}^{(2)}} = \sqrt{\left|\frac{b^{(2)}_{n+1}}{b^{(1)}_{m+1}}\right|},$$

where $b^{(1)}_{m+1}, b^{(2)}_{n+1}$ are the slopes of the last segment and $\mathcal{R}^{(1)}, \mathcal{R}^{(2)}$ are the runup from the bathymetry (1) and (2), respectively. If we define for the kth segment the sloping angle measured with respect to the horizontal axis as, $\beta_k =: \arctan(b_k)$, the previous expression simplifies

$$\frac{\mathcal{R}^{(1)}}{\mathcal{R}^{(2)}} = \sqrt{\left|\frac{\cot(\beta^{(1)}_{n+1})}{\cot(\beta^{(2)}_{m+1})}\right|},$$

which shows that the ratio of the maximum runup of two bathymetries are proportional to the square root of the ratio of the cotangent of the sloping angles of their respective last segments.

For some applications, the bathymetry of a sloping beach is a reasonable first-order approximation of the seabed of a Chilean subduction zone geometry (e.g Fuentes *et al.* 2013). However, our results suggest that one must be careful when modelling tsunamis using a sloping beach setting.

3.4.3 Isosceles N-waves symmetry and runup-rundown modelling

The maximum runup generated by a leading-elevation N wave (LEN) has an analytic closed form which is obtained from complex contour integration, however the maximum runup of a leading-depression N wave (LDN) falls outside of the convergence radius of the series expansion of expression (33). The last reason does not allow us to obtain analytically a closed asymptotic formula for the runup law.

Fig. 5 shows the runup modelling using an incident isosceles LEN and LDN, and their respective time series computed numerically at the shore on a two-linear-segment bathymetry. The water wave elevation evolution at the shore (Fig. 5c) presents an antisymmetrical behaviour

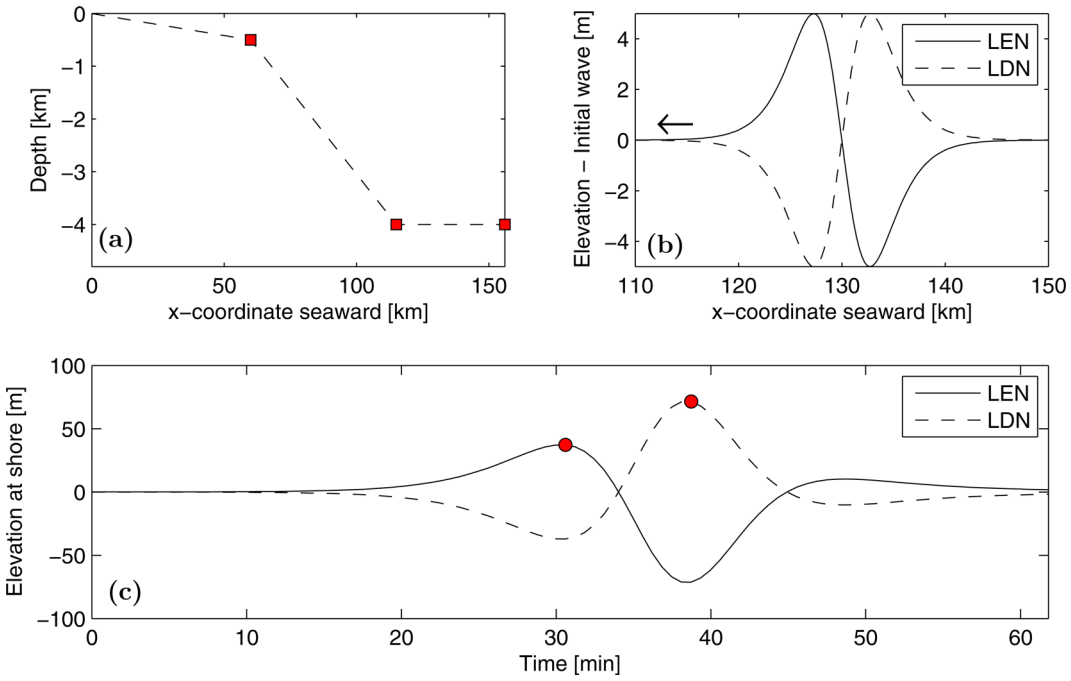

Figure 5. Symmetry observed in the runup evolution in the case of incident isosceles *N* waves. (a) Two linear segments bathymetry. (b) Incident isosceles *N* waves. (c) Runup evolution at the shoreline.

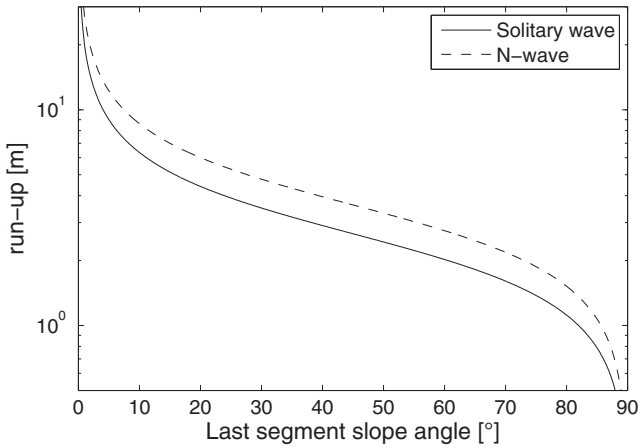

Figure 6. Comparison of the maximum runup computed for an isosceles *N* wave (dashed line) and a solitary wave (solid line), as a function of the sloping angle of the last segment, $n + 1$. Only angles from 0° to 90° are plotted. The seafloor geometry assumes $H = 5$ m and $d = 4$ km.

in terms of their waveforms when comparing the LEN and LDN cases. The LEN has an analytical runup of 39.78 m reached at 30.43 min, which is in very good agreement with the numerical solution, 37.22 m for the maximum runup reached at 30.59 min. The LDN case can only be computed numerically from the integral form and their results are, 71.33 m and 38.70 min, for the maximum runup and runup time, respectively.

Because of the symmetry, the rundown is switched with the runup when comparing LEN and LDN patterns (Fig. 5c). Kânoğlu (2004) also observed this behaviour and also studied different initial conditions for the non-linear shallow water wave equations.

Fig. 6 shows the comparison of the maximum runup generated by both solitary wave and isosceles leading-elevation *N* wave as a function of the sloping angle of the last segment. We assume the same bathymetry, where the runup formula is valid. The incident *N* wave generates systematically a larger runup than the solitary wave, for all angles analysed, however one can observe that the larger differences are for small angles.

3.5 Resonance periods

Because wave amplification can happen on a complex bathymetry, we can use our analytical solution to study the resonance periods of a given seafloor geometry. This phenomena was studied by Ezersky *et al.* (2013) and they obtained a good agreement for observations of the Makran tsunami, excited by the M_w 8.1 1945 Baluchistan earthquake. They set a bathymetry assuming an ocean of constant depth and two

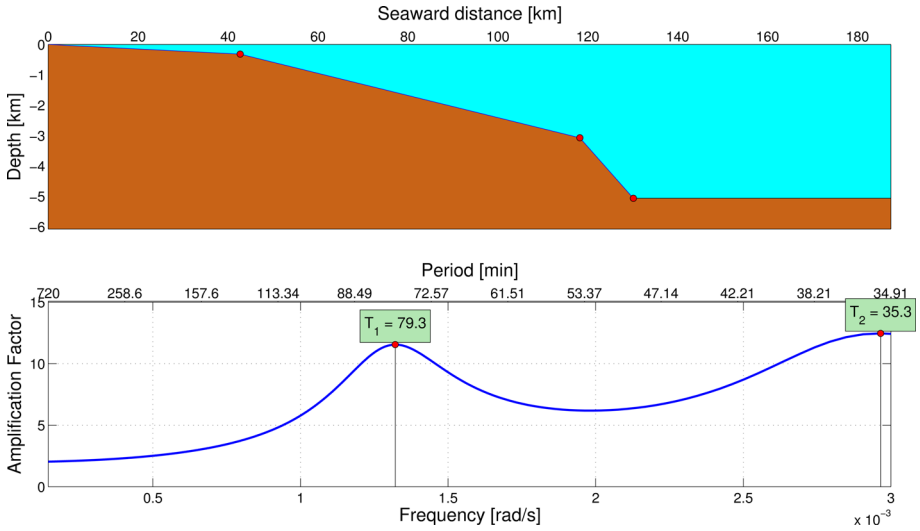

Figure 7. Resonance analysis for (a) three linear segments bathymetry of a Chilean subduction zone and (b) amplification factor as function of frequency predicted by the analytical solution.

linear segments approaching the shore to describe the continental slope and a continental shelf of gentle slope. In our model, because $B_{n+1}(\omega)$ acts like a transfer function, we can use it to estimate the resonance periods at their peaks. We take the values from Ezersky *et al.* (2013) to check our results, and we verified that it produces the same values.

However, because our solution is valid for an arbitrary number of linear segments, we do not need to solve the problem explicitly for a given piecewise bathymetry, but only to specify the propagators for specific bathymetry models.

We study the zone of Constitución (≈35°S) that was hit by the Chilean tsunami in 2010. We adjust a piecewise linear seafloor from the GEBCO bathymmetry by taking the orthogonal transect between the trench and the coastline. Fig. 7 shows the seafloor geometry setup to reproduce the bathymetry of the studied area and compute the resonance periods. We obtain 79 and 35 min for the zero and first mode respectively, which are in agreement with the numerical tsunami study done by Yamazaki & Cheung (2011). Also, at this particular region, the runup formula (45) predicts 29 m, with $H = 5$ (which is approximately the initial wave height at Constitución). This result is in the same order obtained by the runup *in situ* measurements.

4 CONCLUSION

In this work, we present a general mathematical method in order to estimate the water wave elevation for a piecewise bathymetry approximated by linear segments.

We computed theoretically the water wave elevation and runup generated on a piecewise linear bathymetry, by solving the linear shallow water wave equations in the 1+1 dimensional case. We derived a general expression for the runup, assuming an arbitrary number of non-horizontal segments and we developed a specific matrix propagator scheme, similar to the ones used in the propagation of the elastic seismic wave field in a layered medium, such as, the Haskell–Thompson Method (Thomson 1950; Haskell 1953).

We verified analytically the general solution obtained and also its mathematical and physical consistence. In particular, we compared the general solution in the case of one segment and n collinear control points, against the well-known runup solution for the canonical sloping beach model and all solutions agree.

The mathematical approach detailed in this work allowed us to compute analytically an asymptotic closed form for the maximum runup under the assumption of non-horizontal segments and the validity of the asymptotic expansion of the cylindrical Bessel functions for large arguments. We also computed in a closed form the asymptotic expression for the maximum runup on a piecewise linear bathymetry, assuming an incident solitary wave and an isosceles leading-elevation N wave. In contrast to previous analytical studies to compute the runup on piecewise linear bathymetries, we have obtained mathematically a general asymptotic maximum runup formula when n sloping linear segments describe the bathymetry connecting the shore to the ocean of constant depth.

Kânoğlu & Synolakis (1998) developed a general method of solution for the runup allowing horizontal and non-horizontal linear segments in the same bathymetry model. However asymptotic runup computation must be solved for each specific case of bathymetries.

In this sense, the solution proposed in this study generalizes the runup formula when any number of non-horizontal segments are assumed to describe the bathymetry.

As in the sloping beach model, we found that the N wave produces a larger runup than the incident solitary wave case. We found that in both cases, the maximum runup is function of the slope of the last segment approaching the shore, as being basically proportional to $|b_{n+1}|^{-\frac{1}{2}}$.

Analytical verifications and numerical tests were done in order to check the validity of the asymptotic closed expression for the maximum runup and we discussed the validity condition that must be satisfied to get correct solutions. In some cases the asymptotic theoretical solution

fails to predict the exact maximum runup value due to the approximation of Bessel's functions for large argument. Also, it is very important that the inequality that allows to approximate asymptotically the Bessel functions hold valid at each segment, if that is not the case, the runup can not be correctly estimated.

We also applied our model to study the runup on a more realistic bathymetry than a sloping beach model, approximating the seabed of a Chilean subduction zone by two linear segments connected to an ocean of constant depth. The last segment (continental shelf) preserves a gentle slope compared to the continental slope which slopes steeper. Numerical computations were done to compare the runup from both bathymetries assuming an incident solitary wave. Our results shows that a larger runup is produced in a more realistic bathymetry than on a canonical sloping beach case. We discussed the differences in the runup computed numerically from an incident leading-depresion and leading-elevation isosceles *N* wave. These differences are mainly attributed to the symmetry of the initial wave, which produces a pair-relation: runup-LDN = rundown-LEN and runup-LEN = rundown-LDN. Finally, we apply our analytical solution to the calculation of resonance periods and runup heights at Constitución, a small town that was strongly affected by the local Chilean tsunami in 2010. Our numerical results are in agreement with previous studies.

ACKNOWLEDGEMENTS

We would like to thank Professor Armando Cisternas for his guidance and insightful suggestions throughout the progress of this work. We also thank two anonymous reviewers who provided excellent suggestions to improve this manuscript.

REFERENCES

Boussinesq, J., 1871. Théorie de l'intumescence liquide appelée onde solitaire ou de translation, se propageant dans un canal rectangulaire, *Comptes Rendus de l'Academie des Sciences,* **72,** 755–759.

Carrier, G.F. & Greenspan, H.P., 1958. Water waves of finite amplitude on a sloping beach, *J. Fluid Mech.,* **17,** 97–110.

Carrier, G.F., Wu, T.T. & Yeh, H., 2003. Tsunami runup and drawdown on a plane beach, *J. Fluid Mech.,* **475,** 79–99.

Ezersky, A., Tiguercha, D. & Pelinovsky, E., 2013. Resonance phenomena at the long wave run-up on the coast, *Nat. Hazards Earth Syst. Sci.,* **13,** 2745–2752.

Fritz, H.M. *et al.*, 2011. Field survey of the 27 February 2010 Chile tsunami, *Pure appl. Geophys.,* **168,** 1989–2010.

Fuentes, M., Ruiz, J. & Cisternas, A., 2013. A theoretical model of tsunami runup in Chile based on a simple bathymetry, *Geophys. J. Int.,* **196**(2), 986–995.

Fujii, Y., Satake, K., Sakai, S., Shinohara, M. & Kanazawa, T., 2011. Tsunami source of the 2011 off the Pacific coast of Tohoku Earthquake, *Earth Planets Space,* **63,** 815–820.

Haskell, N.A., 1953. The dispersion of surface waves on multilayered media, *Bull. seism. Soc. Am.,* **43,** 17–34.

Hayes, G.P., Bergman, E., Johnson, K.L., Benz, H.M., Brown, L. & Meltzer, A.S., 2013. Seismotectonic framework of the February 27, 2010 Mw 8.8 Maule, Chile earthquake sequence, *Geophys. J. Int.,* **195**(2), 1034–1051.

Ide, S., Baltay, A. & Beroza, G.C., 2011. Shallow dynamic overshoot and energetic deep rupture in the 2011 Mw Tohoku-Oki Earthquake, *Science,* **332,** 1426, doi:10.1126/science.1207020.

Kajiura, K., 1970. Tsunami source, energy and the directivity of wave radiation, *Bull. Earthq. Res. Inst.,* **48,** 835–869.

Kânoğlu, U., 2004. Nonlinear evolution and runup−rundown of long waves over a sloping beach, *J. Fluid Mech.,* **513,** 363–372.

Kânoğlu, U. & Synolakis, C.E., 1998. Long wave runup on piecewise linear topographies, *J. Fluid Mech. (JFM),* **374,** 1–28.

Kânoğlu, U. & Synolakis, C.E., 2006. Initial value problem solution of nonlinear shallow water-wave equations, *Phys. Rev. Lett.,* **97,** 148 501–148 504.

Kânoğlu, U., Titov, V.V., Aydin, B., Moore, C., Stefanakis, T.S., Zhou, H., Spillane, M. & Synolakis, C.E., 2013. Focusing of long waves with finite crest over constant depth, *Proc. R. Soc., A,* **469,** 20130015–20130015.

Lay, T., Ammon, C. J., Kanamori, H., Koper, K.D., Sufri, O. & Hutko, A.R., 2010. Tele-seismic inversion for rupture process of the 27 February 2010 Chile (Mw 8.8) earthquake, *Geophys. Res. Lett.,* **37,** L13301, doi:10.1029/2010GL043379.

Li, Y. & Raichlen, F., 2001. Solitary wave runup on plane slopes, *J. Waterway, Port, Coastal, Ocean Eng.,* **127**(1), 33–44.

Madsen, A., Hemming, A. & Schäffer, 2010. Analytical solutions for tsunami runup on a plane beach: single waves, N-waves and transient waves, *J. Fluid Mech.,* **645,** 27–57.

Mori, N., Takahashi, T., Yasuda, T. & Yanagisawa, H., 2011. Survey of 2011 Tohoku earthquake tsunami inundation and run-up, *Geophys. Res. Lett.,* **38**. L00G14, doi:10.1029/2011GL049210.

Moscoso, E. & Contreras-Reyes, E., 2012. Outer rise seismicity related to the Maule, Chile 2010 megathrust earthquake and hydration of the incoming oceanic lithosphere, *Andean Geol.,* **39**(3), 564–572.

Okal, E.A. & Synolakis, C.E., 2004. Source discrimination for nearfield tsunamis, *Geophys. J. Int.,* **158,** 899–912.

Satake, K. *et al.*, 1993. Tsunami field survey of the 1992 Nicaragua earthquake, *EOS, Trans. Am. geophys. Un.,* **74**(13), 145–156.

Synolakis, C.E., 1986. The runup of long waves. *PhD thesis,* Caltech, Pasadena, California.

Synolakis, C.E., 1987. The runup of solitary waves, *J. Fluid Mech.,* **185,** 523–545.

Synolakis, C.E., 1988. On the roots of $J_0(z) - iJ_1(z)$, *Quater. Appl. Maths.,* **XLVI**(1), 105–108.

Synolakis, C.E., 1991. Tsunami run-up on steep slopes: how good linear theory really is, *Nat. Hazards,* **4,** 221–234.

Tadepalli, S. & Synolakis, C.E., 1994. The run-up on N-waves on sloping beaches, *Proc. R. Soc. Lond., A,* **455,** 99–112.

Tadepalli, S. & Synolakis, C.E., 1996. Model for the leading waves of tsunamis, *Phys. Rev. Lett.,* **77,** 2141–2145.

Tang, L. *et al.*, 2012. Direct energy estimation of the 2011 Japan tsunami using deep-ocean pressure measurements, *J. geophys. Res.,* **117,** C08008, doi:10.1029/2011JC007635.

Thomson, W.T., 1950. Transmission of elastic waves through a stratified solid medium, *J. appl. Phys.,* **21,** 89–93.

Vargas, G., Farías, M., Carretier, S., Tassara, A., Baize, S. & Melnick, D., 2011. Coastal uplift and tsunami effects associated to the 2010 Mw 8.8 Maule earthquake in Central Chile, *Andean Geol.,* **38**(1), 219–238.

Vigny, C. *et al.*, 2011. The 2010 Mw 8.8 Maule megathrust earthquake of Central Chile, monitored by GPS, *Science,* **332,** 1417, doi:10.1126/science.1204132.

Wei, Y., Chamberlin, C., Titov, V., Tang, L. & Bernard, E., 2013. Modeling of the 2011 Japan tsunami: lessons for near-field forecast, *Pure appl. Geophys.,* **170**(6–8), 1309–1331.

Yamazaki, Y. & Cheung, K.F., 2011. Shelf resonance and impact of near-field tsunami generated by the 2010 Chile earthquake, *Geophys. Res. Lett.,* **38,** L12605, doi:10.1029/2011GL047508.

Yamazaki, Y., Kowalik, Z. & Fai Cheung, K., 2009. Depth-integrated, non-hydrostatic model for wave breaking and run-up, *Int. J. Numer. Methods Fluids,* **61**(5), 473–497.

Yeh, H., Imamura, F., Synolakis, C.E., Tsuji, Y., Liu, P.L.-F. & Shi, S., 1993. The Flores Island tsunamis, *EOS, Trans. Am. geophys. Un.,* **74**(33), 369, 371–373.